

Invariants and chaos in the Volterra gyrostat without energy conservation*

Ashwin K Seshadri¹ and S Lakshmivarahan²

¹Centre for Atmospheric and Oceanic Sciences and Divecha Centre for Climate Change, Indian Institute of Science, Bangalore 560012, India. Email: ashwins@iisc.ac.in.

²Emeritus faculty at the School of Computer Science, University of Oklahoma, Norman, OK 73012, USA. Email: varahan@ou.edu.

Declarations of interest: none

*This paper is dedicated to the memory of Professor A S Vasudeva Murthy.

Abstract

The model of the Volterra gyrostat (VG) has not only played an important role in rigid body dynamics but also served as the foundation of low-order models of many naturally occurring systems. It is well known that VG possesses two invariants, or constants of motion, corresponding to kinetic energy and squared angular momentum, giving oscillatory solutions to its equations of motion. Nine distinct subclasses of the VG have been identified, two of which the Euler gyroscope and Lorenz gyrostat are each known to have two constants. This paper characterizes quadratic invariants of the VG and each of its subclasses, showing how these enjoy two invariants even when rendered in terms of a non-invertible transformation of parameters, leading to a transformed Volterra gyrostat (TVG). If the quadratic coefficients of the TVG sum to zero, as they do for the VG, the system conserves energy. In all of these cases, the flows preserve volume. However, physical models where the quadratic coefficients do not sum to zero are ubiquitous, and characterization of invariants and the resulting dynamics for this more general class of models with volume conservation but without energy conservation is lacking. This paper provides the first such characterization for each of the subclasses of the VG in the absence of energy conservation, showing how the number of invariants depends on the number of linear feedback terms. It is shown that the gyrostat with three linear feedback terms has no invariants. The number of invariants circumscribes the possible dynamics for these three-dimensional flows, and those without any invariants are shown to admit rich dynamics including chaos. This gives rise to a broad class of three-dimensional volume conserving chaotic flows, arising naturally from model reduction techniques.

Keywords

Volterra gyrostat; Low-order models; Volume conserving flows; Quadratic invariants; Low-dimensional chaos; Dissipationless limit

1 Introduction

Let $\mathbf{x}(t) = (x_1(t), x_2(t), x_3(t))^T \in \mathbb{R}^3$ be the state of a dynamical system at time $t \geq 0$. Let $\mathbf{f} : \mathbb{R}^3 \rightarrow \mathbb{R}^3$ with $\mathbf{f}(\mathbf{x}) = (f_1(t), f_2(t), f_3(t))^T \in \mathbb{R}^3$ denote the vector field of the associated dynamics where $f_i(\mathbf{x}) = \alpha_i x_j x_k$ for $i \neq j \neq k$ and $\alpha_i \in \mathbb{R}$ for $1 \leq i \leq 3$ satisfy $\alpha_1 + \alpha_2 + \alpha_3 = 0$. Let A denote a skew-symmetric matrix of order 3 having the form

$$A = \begin{bmatrix} 0 & -h_3 & h_2 \\ h_3 & 0 & -h_1 \\ -h_2 & h_1 & 0 \end{bmatrix}. \quad (1)$$

Then

$$\dot{\mathbf{x}}(t) = \mathbf{f}(\mathbf{x}) + A\mathbf{x} \quad (2)$$

describes evolution of the state $\mathbf{x}(t)$ of a dynamical system known as the Volterra gyrostat (VG) [1]. When the matrix $A = 0$ in Eq. (2), the resulting dynamics is called the Euler gyroscope (EG). In the parlance of rigid body dynamics, VG has played a central role in design and control of mechanical systems [2]. More recently it was demonstrated that VG and many of its special cases occur naturally as the basic building blocks to additively construct a variety of low-order, finite dimensional models for many naturally occurring phenomena including the now famous equations of Rayleigh Benard convection [3, 4], vorticity dynamics [5, 6, 7], among others. Refer to [8] (hereafter GT (1999)) and [9, 4, 10]. Many atmospheric low-order models developed through model reduction techniques [11, 12] possess a structure that can be naturally represented as combinations of coupled VGs. The investigation of dynamics in the presence of gyrostatic forces and the resulting integrals of motion is an active area of study [13, 14, 15].

It is well known that VG in Eq. (2) enjoys two invariants: kinetic energy and square of the angular momentum, quadratic invariants that each restrict its trajectories to two manifolds whose intersection is a one-dimensional manifold containing the solution trajectories. By specializing the choice of parameters α_i and h_i , $1 \leq i \leq 3$ in Eq. (2), the authors in GT (1999) identify nine distinct subclasses of VG, which includes the Euler gyroscope (EG), the so-called Lorenz gyrostat (LG), and other nonlinear oscillators. Further extensions of VG that include nonlinear feedback, called generalized VG, are contained in the two papers [16, 17]. For an interesting survey and historical review of the gyrostat and its applications refer to [18].

While it is known (GT (1999)) that among the cases of VG, both the EG and LG enjoy two quadratic invariants, it is not known if the other special cases of VG also possess two invariants. In this brief study, using a common framework, we derive expressions for the two invariants for all the nine special cases of VG. The existence of two quadratic invariants is closely tied to the constraint that the α_i 's sum to zero, which originates in their physical interpretation in terms of the principal moments of inertia of the gyrostat. Furthermore, this constraint plays an important role in energy conservation [17].

It is of interest that there is a close connection between EG and the maximum simplification equations [5, 19]. The systems are not identical, the EG obeys the constraint $\alpha_1 + \alpha_2 + \alpha_3 = 0$, whereas the maximum simplification equations do not. Yet the maximum simplification equations are also known to possess two quadratic invariants. It is not known whether the other special cases of the VG, upon relaxing this constraint, also enjoy two invariants, which in general could differ from those of the VG. Such a property

would give rise to simple oscillatory dynamics, whereas the absence of any invariants is a necessary condition for chaotic behavior in these three-dimensional models.

Prior work has considered the chaotic dynamics resulting from time-varying perturbations to the EG (e.g., [20]). The motivation of the present paper is to analyze the specific models represented by Eqs. (1)-(2), where departures from the EG are state feedback that naturally arise in low-order models from the effects of forcing. A comprehensive analysis for various special cases of Eq. (1)-(2), specializing for various subclasses of the VG [8], is absent.

The approach of this paper allows us to consider the invariants of the VG and its generalization and examine the role played by this constraint. We are thus able to demonstrate that the non-existence of any invariants in these three dimensional flows yields richer dynamics including chaos. Section 2 contains the derivation of the quadratic invariants of the VG, with and without energy conservation. The VG is rendered in a modified form, first described by GT (1999), through a non-invertible transformation of parameters. For each of the subclasses of the resulting system, quadratic invariants are estimated by a common procedure. We consider the effects of removing the constraint $\alpha_1 + \alpha_2 + \alpha_3 = 0$, not only for the maximum simplification equations, but also the eight other subclasses. It is shown that not all of these subclasses possesses two quadratic invariants, giving rise to richer dynamics when this constraint is absent. In the absence of energy conservation, the number of invariants is closely tied to the number of linear feedback terms. Section 3 shows that chaos can arise in those subclasses which do not have any invariants. Thus, we identify new classes of volume conserving chaotic flows that naturally emerge in low-order models without any forcing or dissipation.

2 Constants of motion for the Volterra gyrostat (VG)

2.1 Volterra equations for the gyrostat

Consider Volterra's equations

$$\begin{aligned} K_1^2 \dot{y}_1 &= (K_2^2 - K_3^2) y_2 y_3 + h_2 y_3 - h_3 y_2 \\ K_2^2 \dot{y}_2 &= (K_3^2 - K_1^2) y_3 y_1 + h_3 y_1 - h_1 y_3 \\ K_3^2 \dot{y}_3 &= (K_1^2 - K_2^2) y_1 y_2 + h_1 y_2 - h_2 y_1 \end{aligned} \quad (3)$$

where for $i = 1, 2, 3$, y_i denotes the components of the angular velocity of the carrier body, $K_i^2 = I_i$ are the principal moments of inertia of the gyrostat, and h_i are the components of the fixed angular momentum of the rotor relative to the carrier. The dots indicate rate of change, for e.g., $\dot{y}_1 = dy_1/dt$. Together these constitute the gyrostat, which possesses two quadratic invariants, the kinetic energy

$$E = \frac{1}{2} \sum_{i=1}^3 K_i^2 y_i^2 \quad (4)$$

and the magnitude of the angular momentum vector, or equivalently one-half of its square

$$M = \frac{1}{2} \sum_{i=1}^3 \left(K_i^2 y_i + h_i \right)^2 \quad (5)$$

both of which are constant in time for Eq. (3), i.e., $\dot{E} = \dot{M} = 0$ (GT (1999)).

2.2 Transformed Volterra gyrostat (TVG)

Consider transformation of variables $K_i y_i = x_i$, introduced by GT (1999). In state variables x_i , the gyrostat equations are

$$\begin{aligned} K_1 K_2 K_3 \dot{x}_1 &= \left(K_2^2 - K_3^2 \right) x_2 x_3 + K_2 h_2 x_3 - K_3 h_3 x_2 \\ K_1 K_2 K_3 \dot{x}_2 &= \left(K_3^2 - K_1^2 \right) x_3 x_1 + K_3 h_3 x_1 - K_1 h_1 x_3 \\ K_1 K_2 K_3 \dot{x}_3 &= \left(K_1^2 - K_2^2 \right) x_1 x_2 + K_1 h_1 x_2 - K_2 h_2 x_1 \end{aligned} \quad (6)$$

and, defining a new time-variable $t = K_1 K_2 K_3 s$, so that

$$\frac{d}{ds} = \frac{d}{dt} \frac{dt}{ds} = K_1 K_2 K_3 \frac{d}{dt} \quad (7)$$

we obtain

$$\begin{aligned} x'_1 &= \left(K_2^2 - K_3^2 \right) x_2 x_3 + K_2 h_2 x_3 - K_3 h_3 x_2 \\ x'_2 &= \left(K_3^2 - K_1^2 \right) x_3 x_1 + K_3 h_3 x_1 - K_1 h_1 x_3 \\ x'_3 &= \left(K_1^2 - K_2^2 \right) x_1 x_2 + K_1 h_1 x_2 - K_2 h_2 x_1 \end{aligned} \quad (8)$$

where $'$ denotes d/ds . This model satisfies $M' = dM/ds = 0$. Defining new parameters

$$\begin{aligned} p &= K_2^2 - K_3^2, q = K_3^2 - K_1^2, \text{ and } r = K_1^2 - K_2^2 \\ a &= K_1 h_1, b = K_2 h_2, \text{ and } c = K_3 h_3 \end{aligned} \quad (9)$$

with $p + q + r = 0$, the model is rendered as

$$\begin{aligned} x'_1 &= p x_2 x_3 + b x_3 - c x_2 \\ x'_2 &= q x_3 x_1 + c x_1 - a x_3 \\ x'_3 &= r x_1 x_2 + a x_2 - b x_1, \end{aligned} \quad (10)$$

which we denote as the transformed Volterra gyrostat (TVG). The quadratic invariants of this model will be considered in the remainder of this section. The symbols used in the paper are summarized in Table 4.

2.3 Constants of motion of TVG

Since the transformation in Eq. (6) is smooth, we expect TVG to possess as many constants of motion (“invariants”) as VG, as is easily shown. A system

$$\dot{\mathbf{y}} = \mathbf{g}(\mathbf{y}) \quad (11)$$

with $\mathbf{y} = [y_1 \ y_2 \ \dots \ y_n]^T \in \mathbb{R}^n$ being the state vector and $\mathbf{g} = [g_1 \ g_2 \ \dots \ g_n]^T : \mathbb{R}^n \rightarrow \mathbb{R}^n$ the vector field has k distinct invariants $C_i(y_1, y_2, \dots, y_n)$ if

$$\frac{dC_i}{dt} = \sum_{j=1}^n \frac{\partial C_i}{\partial y_j} \dot{y}_j = 0 \quad (12)$$

for $i = 1, 2, \dots, k$. Now, if there is a smooth change of variables $\mathbf{y} = \mathbf{h}(\mathbf{x})$, where $\mathbf{h} = [h_1 \ h_2 \ \dots \ h_n]^T : \mathbb{R}^n \rightarrow \mathbb{R}^n$ we have

$$\dot{y}_j = \sum_{l=1}^n \frac{\partial h_j}{\partial x_l} \dot{x}_l \quad (13)$$

and substituting in Eq. (12)

$$\frac{dC_i}{dt} = \sum_{l=1}^n \left(\sum_{j=1}^n \frac{\partial C_i}{\partial y_j} \frac{\partial h_j}{\partial x_l} \right) \dot{x}_l = 0 \quad (14)$$

for $i = 1, 2, \dots, k$, such that any smooth change of variables must preserve the invariants. Thus, for kinetic energy

$$E = \frac{1}{2} \sum_{i=1}^3 K_i^2 \left(\frac{x_i}{K_i} \right)^2 = \frac{1}{2} \sum_{i=1}^3 x_i^2 \quad (15)$$

its evolution

$$E' = \sum x_i x_i' = 0 \quad (16)$$

from Eq. (10), since $p + q + r = 0$. Similarly, for the angular momentum

$$M = \frac{1}{2} \sum_{i=1}^3 (K_i x_i + h_i)^2 \quad (17)$$

we obtain

$$M' = \sum_{i=1}^3 (K_i x_i + h_i) K_i x_i' \quad (18)$$

and, upon substituting from Eq. (10)

$$M' = x_1 x_2 x_3 \left(K_1^2 p + K_2^2 q + K_3^2 r \right) + c x_1 x_2 \left(r + K_2^2 - K_1^2 \right) + a x_2 x_3 \left(p + K_3^2 - K_2^2 \right) + b x_1 x_3 \left(q + K_1^2 - K_3^2 \right) \quad (19)$$

and, using the relations in Eq. (9), we obtain also

$$M' = 0. \quad (20)$$

There is an incongruity in the above analysis leading to Eq. (20), with Eq. (19) containing parameters of the VG as well as the TVG. In general, we know the representation of the model in either one set of variables, the VG or the TVG, but not both. This would not be a cause for difficulty if, given the TVG in Eq. (10), we were to solve for the parameters including K_i , $i = 1, 2, 3$ of the VG. However, this parameter transformation is not invertible, as shown below. Consider Jacobian

$$H \equiv \begin{bmatrix} \frac{\partial p}{\partial K_1} & \frac{\partial p}{\partial K_2} & \frac{\partial p}{\partial K_3} & \frac{\partial p}{\partial h_1} & \frac{\partial p}{\partial h_2} & \frac{\partial p}{\partial h_3} \\ \frac{\partial q}{\partial K_1} & \frac{\partial q}{\partial K_2} & \frac{\partial q}{\partial K_3} & \frac{\partial q}{\partial h_1} & \frac{\partial q}{\partial h_2} & \frac{\partial q}{\partial h_3} \\ \frac{\partial r}{\partial K_1} & \frac{\partial r}{\partial K_2} & \frac{\partial r}{\partial K_3} & \frac{\partial r}{\partial h_1} & \frac{\partial r}{\partial h_2} & \frac{\partial r}{\partial h_3} \\ \frac{\partial a}{\partial K_1} & \frac{\partial a}{\partial K_2} & \frac{\partial a}{\partial K_3} & \frac{\partial a}{\partial h_1} & \frac{\partial a}{\partial h_2} & \frac{\partial a}{\partial h_3} \\ \frac{\partial b}{\partial K_1} & \frac{\partial b}{\partial K_2} & \frac{\partial b}{\partial K_3} & \frac{\partial b}{\partial h_1} & \frac{\partial b}{\partial h_2} & \frac{\partial b}{\partial h_3} \\ \frac{\partial c}{\partial K_1} & \frac{\partial c}{\partial K_2} & \frac{\partial c}{\partial K_3} & \frac{\partial c}{\partial h_1} & \frac{\partial c}{\partial h_2} & \frac{\partial c}{\partial h_3} \end{bmatrix} \quad (21)$$

which is

$$H = \begin{bmatrix} 0 & 2K_2 & -2K_3 & 0 & 0 & 0 \\ -2K_1 & 0 & 2K_3 & 0 & 0 & 0 \\ 2K_1 & -2K_2 & 0 & 0 & 0 & 0 \\ h_1 & 0 & 0 & K_1 & 0 & 0 \\ 0 & h_2 & 0 & 0 & K_2 & 0 \\ 0 & 0 & h_3 & 0 & 0 & K_3 \end{bmatrix}. \quad (22)$$

The determinant of this matrix

$$\det H = K_1 K_2 K_3 \det \begin{bmatrix} 0 & 2K_2 & -2K_3 \\ -2K_1 & 0 & 2K_3 \\ 2K_1 & -2K_2 & 0 \end{bmatrix} = 0 \quad (23)$$

and the transformation of parameters in Eq. (9) is not invertible, since the rows and columns of the matrix in Eq. (23) are linearly dependent. Thus K_1, K_2, K_3 cannot be determined from knowledge of p, q, r .

2.4 Estimating the quadratic invariants

Owing to this, it remains to recover directly the invariants of the TVG in Eq. (10). Consider the more general problem of finding quadratic invariants, given a vector field. We consider quadratic invariants only, since any invariants must be closely tied to those of the VG. As for the VG, these can only be identified up to affine transformations, giving us families of invariants. We consider general quadratic functions

$$C(x_1, x_2, x_3) = \frac{1}{2}d_{200}x_1^2 + \frac{1}{2}d_{020}x_2^2 + \frac{1}{2}d_{002}x_3^2 + d_{110}x_1x_2 + d_{011}x_2x_3 + d_{101}x_1x_3 + d_{100}x_1 + d_{010}x_2 + d_{001}x_3. \quad (24)$$

For C constant in time

$$C' = \frac{\partial C}{\partial x_1} x_1' + \frac{\partial C}{\partial x_2} x_2' + \frac{\partial C}{\partial x_3} x_3' = 0 \quad (25)$$

and, differentiating Eq. (24) and substituting for the vector field and collecting terms

$$\begin{aligned} C' = & (d_{200}p + d_{020}q + d_{002}r) x_1 x_2 x_3 + d_{110}p x_2^2 x_3 + d_{101}p x_2 x_3^2 + d_{110}q x_3 x_1^2 + d_{011}q x_3^2 x_1 + d_{011}r x_1 x_2^2 + d_{101}r x_1^2 x_2 \\ & + (-d_{200}c + d_{020}c + d_{101}a - d_{011}b + d_{001}r) x_1 x_2 + (-d_{020}a + d_{002}a + d_{110}b - d_{101}c + d_{100}p) x_2 x_3 \\ & + (-d_{002}b + d_{200}b + d_{011}c - d_{110}a + d_{010}q) x_3 x_1 + (-d_{101}b + d_{110}c) x_1^2 + (-d_{110}c + d_{011}a) x_2^2 + (-d_{011}a + d_{101}b) x_3^2 \\ & + (-d_{001}b + d_{010}c) x_1 + (-d_{100}c + d_{001}a) x_2 + (-d_{010}a + d_{100}b) x_3 = 0. \end{aligned} \quad (26)$$

Since each of the terms are linearly independent in time, all coefficients in the above equation must vanish. Considering first the coefficients of $x_2^2 x_3$ and $x_3 x_1^2$, we have

$$d_{110}p = d_{110}q = 0. \quad (27)$$

If both p and q were zero, then $r = 0$, owing to the energy-conserving constraint $p + q + r = 0$. Such a model is linear, and excluding such linear models from consideration leads to $d_{110} = 0$. Similarly, we have also $d_{101} = d_{011} = 0$, and constants of motion of the TVG do not possess mixed quadratic terms such as $x_1 x_2$ etc. Thus we are led to the following equations for parameters in Eq. (24), in matrix vector form

$$\begin{bmatrix} p & q & r & 0 & 0 & 0 \\ -c & c & 0 & 0 & 0 & r \\ 0 & -a & a & p & 0 & 0 \\ b & 0 & -b & 0 & q & 0 \\ 0 & 0 & 0 & 0 & c & -b \\ 0 & 0 & 0 & -c & 0 & a \\ 0 & 0 & 0 & b & -a & 0 \end{bmatrix} \begin{bmatrix} d_{200} \\ d_{020} \\ d_{002} \\ d_{100} \\ d_{010} \\ d_{001} \end{bmatrix} = \begin{bmatrix} 0 \\ 0 \\ 0 \\ 0 \\ 0 \\ 0 \end{bmatrix} \quad (28)$$

or,

$$Bd = 0 \quad (29)$$

where $B \in \mathbb{R}^{7 \times 6}$ and $d = [d_{200} \ d_{020} \ d_{002} \ d_{100} \ d_{010} \ d_{001}]^T$. That is, $d \in \text{NULL}(B)$, and the number of independent quadratic invariants is governed by the dimension of $\text{NULL}(B)$. For two quadratic invariants to exist, we must have $\dim(\text{NULL}(B)) = 2$. From the rank-nullity theorem, $\dim(\text{NULL}(B)) + \dim(\text{RANGE}(B)) = 6$, so two quadratic invariants are inconsistent with more than 4 linearly independent rows (or columns) of the matrix B .

General case

We first treat the general case, with all of p, q, r, a, b, c being non-zero. From the last two equations

$$\begin{aligned} d_{010} &= \frac{b}{a} d_{100} \\ d_{001} &= \frac{c}{a} d_{100} \end{aligned} \quad (30)$$

and substituting these into the fourth equation

$$d_{002} = d_{200} + \frac{q}{a} d_{100}. \quad (31)$$

The second equation yields

$$\begin{aligned} d_{020} &= d_{200} - \frac{r}{c} d_{001} = d_{200} - \frac{r}{a} d_{100} \\ &= d_{200} + \frac{p+q}{a} d_{100} \end{aligned} \quad (32)$$

where we have used Eq. (30) and $p+q+r=0$. The first, third, and fifth equations are linearly dependent with these that have been used. Using these relations, the invariants are of the form

$$\begin{aligned} C(x_1, x_2, x_3) &= \frac{1}{2} d_{200} x_1^2 + \frac{1}{2} d_{020} x_2^2 + \frac{1}{2} d_{002} x_3^2 + d_{100} x_1 + d_{010} x_2 + d_{001} x_3 \\ &= \frac{1}{2} d_{200} x_1^2 + \frac{1}{2} \left(d_{200} + \frac{p+q}{a} d_{100} \right) x_2^2 + \frac{1}{2} \left(d_{200} + \frac{q}{a} d_{100} \right) x_3^2 + d_{100} x_1 + \frac{b}{a} d_{100} x_2 + \frac{c}{a} d_{100} x_3 \end{aligned} \quad (33)$$

and rewritten in terms of d_{200} and d_{100}

$$C(x_1, x_2, x_3) = \frac{1}{2} d_{200} (x_1^2 + x_2^2 + x_3^2) + d_{100} \left(\frac{p+q}{2a} x_2^2 + \frac{q}{2a} x_3^2 + x_1 + \frac{b}{a} x_2 + \frac{c}{a} x_3 \right). \quad (34)$$

Thus, the two invariants are

$$C_1(x_1, x_2, x_3) = \frac{1}{2} (x_1^2 + x_2^2 + x_3^2), \quad (35)$$

which is kinetic energy, and

$$C_2(x_1, x_2, x_3) = \frac{p+q}{2a} x_2^2 + \frac{q}{2a} x_3^2 + x_1 + \frac{b}{a} x_2 + \frac{c}{a} x_3, \quad (36)$$

which is related to the angular momentum squared as shown below. Substituting $K_i y_i = x_i$ and Eqs. (9) above

$$C_2 = \frac{K_2^2 - K_1^2}{2K_1 h_1} K_2^2 y_2^2 + \frac{K_3^2 - K_1^2}{2K_1 h_1} K_3^2 y_3^2 + K_1 y_1 + \frac{K_2 h_2}{K_1 h_1} K_2 y_2 + \frac{K_3 h_3}{K_1 h_1} K_3 y_3 \quad (37)$$

which can be written as

$$K_1 h_1 C_2 = \frac{1}{2} (K_1^2 y_1 + h_1)^2 + \frac{1}{2} (K_2^2 y_2 + h_2)^2 + \frac{1}{2} (K_3^2 y_3 + h_3)^2 - K_1^2 \left(\frac{K_1^2 y_1^2 + K_2^2 y_2^2 + K_3^2 y_3^2}{2} \right) - (h_1^2 + h_2^2 + h_3^2)$$

and therefore

$$K_1 h_1 C_2 = M - K_1^2 E - \left(h_1^2 + h_2^2 + h_3^2 \right). \quad (38)$$

Since $\dot{C}_2 = \dot{M} - K_1^2 \dot{E} = 0$, we have both $\dot{M} = \dot{E} = 0$, that is angular momentum and kinetic energy are conserved in the TVG, as in the VG.

Subclasses of the TVG

Further subclasses of the TVG, wherein one or more of its parameters p, q, r, a, b, c are zero, have been distinguished by GT (1999). From the constraint that $p + q + r = 0$, at least two of the quadratic coefficients must be nonzero for the TVG to indeed be nonlinear. Thus, owing to the symmetries in the model, the authors have focused on the situation with $r = 0$, since the cases with either $p = 0$ or $q = 0$ are analogous. This yields nine distinct subclasses, whose constants of motion are summarized in this section (see Table 1). Further details of the calculation are provided in the Supplementary Information (SI). This model has two free parameters in Eq. (24) (SI Table 1) and thus two independent quadratic invariants (Table 1), for each subclass. Furthermore, in every subclass of this model, $\frac{1}{2} (x_1^2 + x_2^2 + x_3^2)$ is constant. This corresponds to energy conservation in the TVG. Analysis of the last two degenerate cases where $x_3' = 0$ is found in the SI.

The existence of these two quadratic invariants is guaranteed by properties of the matrix \mathbf{B} in Eq. (30). For example, it can be shown that three rows (e.g. the first, third, and fifth) are linearly dependent with the others. For the non-degenerate cases the rank of this matrix is the number of independent rows, i.e. 4. The rank and the dimension of its null-space must sum to 6, the number of independent parameters we seek to estimate for the invariants. Thus the null-space is two-dimensional, and there are two constants of motion in general for this model. A similar conclusion is found for the degenerate cases (SI). These constants of motion correspond to surfaces denoted as \mathcal{C}_1 and \mathcal{C}_2 , which are plotted in Figures 1 and 2, for the subclasses and full model respectively. In summary, we have found two quadratic invariants for all variants of the TVG, rooted in the physics of the VG itself.

Table 1: Expressions for constants of motion of the TVG in Eq. (10). In each subclass, $\frac{1}{2}(x_1^2 + x_2^2 + x_3^2)$ is conserved.

No.	Subclass	C_1	C_2
1	$r = 0; b = c = 0$	$\frac{1}{2}(x_1^2 + x_2^2 + x_3^2)$	$\frac{q}{2a}x_3^2 + x_1$
2	$r = 0; c = 0$	$\frac{1}{2}(x_1^2 + x_2^2 + x_3^2)$	$\frac{q}{2a}x_3^2 + x_1 + \frac{b}{a}x_2$
3	$r = 0; b = 0$	$\frac{1}{2}(x_1^2 + x_2^2 + x_3^2)$	$\frac{q}{2a}x_3^2 + x_1 + \frac{c}{a}x_3$
4	$r = 0$	$\frac{1}{2}(x_1^2 + x_2^2 + x_3^2)$	$\frac{q}{2a}x_3^2 + x_1 + \frac{b}{a}x_2 + \frac{c}{a}x_3$
5	$a = b = c = 0$	$\frac{1}{2}\left(x_1^2 + \frac{p}{p+q}x_3^2\right)$	$\frac{1}{2}\left(x_2^2 + \frac{q}{p+q}x_3^2\right)$
6	$b = c = 0$	$\frac{1}{2}\left(x_1^2 + \frac{p}{p+q}x_3^2 - \frac{2a}{p+q}x_1\right)$	$\frac{1}{2}\left(x_2^2 + \frac{q}{p+q}x_3^2 + \frac{2a}{p+q}x_1\right)$
7	$c = 0$	$\frac{1}{2}\left(x_1^2 + \frac{p}{p+q}x_3^2 - \frac{2a}{p+q}x_1 - \frac{2b}{p+q}x_2\right)$	$\frac{1}{2}\left(x_2^2 + \frac{q}{p+q}x_3^2 + \frac{2a}{p+q}x_1 + \frac{2b}{p+q}x_2\right)$
8	$r = 0; a = b = c = 0$	$\frac{1}{2}(x_1^2 + x_2^2)$	$\frac{1}{2}x_3^2$
9	$r = 0; a = b = 0$	$\frac{1}{2}(x_1^2 + x_2^2)$	$\frac{1}{2}x_3^2$

The intersection of the two-dimensional surfaces \mathcal{C}_1 , \mathcal{C}_2 is a one dimensional manifold, giving oscillatory periodic solutions if q, p have opposite sign. We have solved for the implicit functions describing these trajectories, in Table 2. The numerically integrated solutions are plotted as solid black curves in SI Figures 1 and 2, where we have taken p, q to have opposite sign. SI Fig 1 shows the periodic nature of the solutions with time, for the different subclasses of the model and corresponding constants of motion are plotted versus time in SI Fig 2, confirming their nature. SI Table 2 lists the fixed points of these equations and their stability. Each of the fixed points has a zero eigenvalue so, by the theorem of Hartman and Grobman [21], the nonlinear dynamics cannot be inferred from a linearized stability analysis.

Table 2: Intersections of the two constants of motion of the TVG, yielding oscillatory solution curves since p, q are of opposite sign.

No.	Subclass	$\mathcal{C}_1 \cap \mathcal{C}_2$
1	$r = 0; b = c = 0$	$\frac{1}{2} \left\{ \left(x_1 - \frac{a}{q} \right)^2 + x_2^2 \right\} = C_1 - \frac{a}{q} C_2 + \frac{1}{2} \frac{a^2}{q^2}$
2	$r = 0; c = 0$	$\frac{1}{2} \left\{ \left(x_1 - \frac{a}{q} \right)^2 + \left(x_2 - \frac{b}{q} \right)^2 \right\} = C_1 - \frac{a}{q} C_2 + \frac{1}{2} \frac{a^2 + b^2}{q^2}$
3	$r = 0; b = 0$	$\frac{1}{2} \left\{ \left(\frac{q}{2a} x_3^2 + \frac{c}{a} x_3 - C_2 \right)^2 + x_2^2 + x_3^2 \right\} = C_1$
4	$r = 0$	$\frac{1}{2} \left\{ \left(\frac{q}{2a} x_3^2 + \frac{b}{a} x_2 + \frac{c}{a} x_3 - C_2 \right)^2 + x_2^2 + x_3^2 \right\} = C_1$
5	$a = b = c = 0$	$\frac{1}{2} \left(x_2^2 - \frac{q}{p} x_1^2 \right) = -\frac{q}{p} C_1 + C_2$
6	$b = c = 0$	$\frac{1}{2} \left(\frac{p-q}{2p} x_1^2 + x_2^2 + \frac{a}{p} x_1 \right) = \frac{p-q}{2p} C_1 + C_2$
7	$c = 0$	$\frac{1}{2} \left(\frac{p-q}{2p} x_1^2 + x_2^2 + \frac{a}{p} x_1 + \frac{b}{p} x_2 \right) = \frac{p-q}{2p} C_1 + C_2$
8	$r = 0; a = b = c = 0$	$\frac{1}{2} (x_1^2 + x_2^2) = C_1$
9	$r = 0; a = b = 0$	$\frac{1}{2} (x_1^2 + x_2^2) = C_1$

2.5 Role of energy conservation

The TVG possesses two constants of motion, corresponding to kinetic energy and squared angular momentum. Any linear combination of these quantities, together with an affine transformation, is conserved, i.e.

$$\alpha_1 E + \alpha_2 M + \alpha_3 \tag{39}$$

is constant, for any $\alpha_1, \alpha_2, \alpha_3 \in \mathbb{R}$. This is because the transformation of state variables from the VG to the TVG is smooth. Although the constants of motion of the TVG can be related to those of the VG, they are not naturally rendered as such (Table 1), owing to the non-invertibility of parameters in going from VG to TVG. An important constraint in the above discussion is $p + q + r = 0$, arising from the inextricable link between these parameters and the moments of inertia, as Eq. (9) shows. If the TVG is rooted in the physics of the VG, then it must conserve kinetic energy. As described by [17], energy conserving LOMs must obey this constraint.

It is useful to examine models that have the form given in Eq. (10), yet do not conserve energy. Many LOMs possess this structure, even where they do not satisfy energy conservation, for example Lorenz's maximum simplification equations [5, 19] resemble the Euler gyroscope (subclass 5 in Table 2) with the

difference being that in Lorenz's model $p + q + r \neq 0$. Although these equations do not conserve kinetic energy, they are known to enjoy two invariants [19]. In the case of this model none of the invariants correspond to kinetic energy of the gyrostat, which is obviously not conserved. Yet, it is clear from the equations that the flow conserves volume, since the trace of the Jacobian of the vector field of the TVG

$$\begin{bmatrix} \frac{\partial x_1'}{\partial x_1} & \frac{\partial x_1'}{\partial x_2} & \frac{\partial x_1'}{\partial x_3} \\ \frac{\partial x_2'}{\partial x_1} & \frac{\partial x_2'}{\partial x_2} & \frac{\partial x_2'}{\partial x_3} \\ \frac{\partial x_3'}{\partial x_1} & \frac{\partial x_3'}{\partial x_2} & \frac{\partial x_3'}{\partial x_3} \end{bmatrix} = \begin{bmatrix} 0 & px_3 - c & px_2 + b \\ qx_3 + c & 0 & qx_1 - a \\ rx_2 - b & rx_1 + a & 0 \end{bmatrix} \quad (40)$$

is zero, regardless of whether energy is conserved. However volume conservation does not assure the existence of constants of motion. This is evaluated further for those variants of the TVG that do not conserve kinetic energy for which, in analogy with the subclasses defined by [8], we limit our present analysis to models possessing two or more quadratic terms.

General case

The most general TVG without energy conservation possesses no other constants of motion, as shown below. From Eq. (26), we first consider the part arising from mixed quadratic terms in the constants of motion

$$d_{110} \left(px_2^2 x_3 + qx_3 x_1^2 \right) + d_{101} \left(px_2 x_3^2 + rx_1^2 x_2 \right) + d_{011} \left(qx_3^2 x_1 + rx_1 x_2^2 \right) = 0 \quad (41)$$

where the last equality holds because these terms are linearly independent of the others. Since there are at least two quadratic terms, more than one of p, q, r is non-zero. Then, we cannot in general have $px_2^2 x_3 + qx_3 x_1^2 = 0$ and therefore $d_{110} = 0$. Similarly, $d_{101} = d_{011} = 0$. Here too there cannot be any mixed quadratic terms in the quadratic constants of motion.

Thus, we are left with the same system of equations as before for the parameters

$$\begin{aligned} d_{200}p + d_{020}q + d_{002}r &= 0 \\ -d_{200}c + d_{020}c + d_{001}r &= 0 \\ -d_{020}a + d_{002}a + d_{100}p &= 0 \\ d_{200}b - d_{002}b + d_{010}q &= 0 \\ d_{010}c - d_{001}b &= 0 \\ -d_{100}c + d_{001}a &= 0 \\ d_{100}b - d_{010}a &= 0 \end{aligned} \quad (42)$$

with the difference that that $p + q + r \neq 0$. From the last two equations, we obtain as before

$$\begin{aligned} d_{010} &= \frac{b}{a} d_{100} \\ d_{001} &= \frac{c}{a} d_{100}, \end{aligned} \quad (43)$$

while the fifth equation is linearly dependent as before. Substituting into the fourth equation we obtain

$$d_{002} = d_{200} + \frac{q}{b}d_{010} = d_{200} + \frac{q}{a}d_{100} \quad (44)$$

and from the second equation

$$d_{020} = d_{200} - \frac{r}{c}d_{001} = d_{200} - \frac{r}{a}d_{100}. \quad (45)$$

The third equation yields

$$-\left(d_{200} - \frac{r}{a}d_{100}\right)a + \left(d_{200} + \frac{q}{a}d_{100}\right)a + d_{100}p = 0 \quad (46)$$

or equivalently

$$(p + q + r)d_{100} = 0. \quad (47)$$

If $p + q + r \neq 0$ then $d_{100} = 0$ and, from Eq. (43), $d_{010} = d_{001} = 0$. Furthermore, we also obtain, from Eqs. (44)-(45), $d_{002} = d_{020} = d_{200}$. Then, from the first equation

$$(p + q + r)d_{200} = 0 \quad (48)$$

or, $d_{200} = 0$, and therefore also $d_{020} = d_{002} = 0$. Thus, in the absence of energy conservation, there are no constants of motion in the general case.

Maximum simplification equations

The above discussion assumed that $a, b, c \neq 0$. Let us repeat the above analysis for Lorenz's maximum simplification equations where $a = b = c = 0$ and $p + q + r \neq 0$ with moreover $p, q, r \neq 0$. The equations for the coefficients become

$$\begin{aligned} d_{200}p + d_{020}q + d_{002}r &= 0 \\ d_{001}r &= 0 \\ -d_{100}p &= 0 \\ d_{010}q &= 0 \end{aligned}$$

yielding $d_{100} = d_{010} = d_{001} = 0$ and

$$d_{200}p + d_{020}q + d_{002}r = 0 \quad (49)$$

for one constraint in $d_{200}, d_{020}, d_{002}$. Thus, there are two constants of motion for this model possessing only quadratic terms. The maximum simplification equations have [19]

$$\begin{aligned} p &= - \left(\frac{1}{k^2} - \frac{1}{l^2 + k^2} \right) kl \\ q &= \left(\frac{1}{l^2} - \frac{1}{l^2 + k^2} \right) kl \\ r &= -\frac{1}{2} \left(\frac{1}{l^2} - \frac{1}{k^2} \right) kl \end{aligned} \quad (50)$$

with

$$p + q + r = \frac{1}{2} \left(\frac{1}{l^2} - \frac{1}{k^2} \right) kl \neq 0 \quad (51)$$

since $l \neq k$. For this case two quadratic invariants have been identified

$$E = \frac{1}{4} \left(\frac{A^2}{l^2} + \frac{F^2}{k^2} + \frac{2}{k^2 + l^2} G^2 \right) \quad (52)$$

and

$$V = \frac{1}{2} \left(A^2 + F^2 + 2G^2 \right) \quad (53)$$

where, A, F, G are the state variables [5]. Each of these invariants satisfy $d_{100} = d_{010} = d_{001} = 0$. In the first case

$$d_{200} = \frac{1}{2l^2}; d_{020} = \frac{1}{2k^2}; d_{002} = \frac{1}{k^2 + l^2} \quad (54)$$

so that

$$d_{200}p + d_{020}q + d_{002}r = \left\{ -\frac{1}{2l^2} \left(\frac{1}{k^2} - \frac{1}{l^2 + k^2} \right) + \frac{1}{2k^2} \left(\frac{1}{l^2} - \frac{1}{l^2 + k^2} \right) - \frac{1}{2} \frac{1}{k^2 + l^2} \left(\frac{1}{l^2} - \frac{1}{k^2} \right) \right\} kl = 0. \quad (55)$$

Similarly, in the second case

$$d_{200} = 1; d_{020} = 1; d_{002} = 2 \quad (56)$$

so that

$$d_{200}p + d_{020}q + d_{002}r = \left\{ - \left(\frac{1}{k^2} - \frac{1}{l^2 + k^2} \right) + \left(\frac{1}{l^2} - \frac{1}{l^2 + k^2} \right) - \left(\frac{1}{l^2} - \frac{1}{k^2} \right) \right\} kl = 0. \quad (57)$$

Thus the maximum simplification equations, together with the more general subclass of which they are a part, exhibit oscillatory solutions.

Subclasses of the TVG

The previous two sections demonstrated that whenever there is energy conservation in the TVG, these equations also enjoy a second constant of motion. This leads to oscillatory solutions, for each of the nine subclasses of the TVG as well as the general case where all parameters are nonzero. In the absence of energy conservation, this is not the case and the dynamics admit richer possibilities. To show this, we

list the quadratic invariants for the nine different subclasses in Table 3 (details in SI). Recall that the general case possesses no quadratic invariants. Without energy conservation, for the different subclasses the number of such invariants ranges from zero to two. The last two degenerate subclasses possess two independent constants (SI).

- Two invariants are enjoyed by those subclasses having either $a = b = c = 0$ or $b = c = 0$, or $a = b = 0$ for the degenerate cases (Table 3). These subclasses are the ones containing at most a single linear coefficient. For example $b = c = 0$ simplifies the equations for the coefficients

$$\begin{bmatrix} p & q & r & 0 & 0 & 0 \\ 0 & 0 & 0 & 0 & 0 & r \\ 0 & -a & a & p & 0 & 0 \\ 0 & 0 & 0 & 0 & q & 0 \\ 0 & 0 & 0 & 0 & 0 & a \\ 0 & 0 & 0 & 0 & -a & 0 \end{bmatrix} \begin{bmatrix} d_{200} \\ d_{020} \\ d_{002} \\ d_{001} \\ d_{010} \\ d_{001} \end{bmatrix} = \begin{bmatrix} 0 \\ 0 \\ 0 \\ 0 \\ 0 \\ 0 \end{bmatrix} \quad (58)$$

so $d_{010} = d_{001} = 0$, which leaves two independent equations

$$\begin{aligned} d_{200}p + d_{020}q + d_{002}r &= 0 \\ -d_{020}a + d_{002}a + d_{100}p &= 0 \end{aligned} \quad (59)$$

in four unknowns, making for two independent invariants. With each of $a = b = c = 0$ this situation remains basically the same, leading to the subclass that corresponds to Lorenz's maximum simplification equations, which, as noted earlier, has periodic solutions.

- Table 3 shows that a single constant of motion is held by subclasses of the model having two nonzero linear coefficients. For example with $c = 0$ the equations become

$$\begin{bmatrix} p & q & r & 0 & 0 & 0 \\ 0 & 0 & 0 & 0 & 0 & r \\ 0 & -a & a & p & 0 & 0 \\ b & 0 & -b & 0 & q & 0 \\ 0 & 0 & 0 & 0 & 0 & -b \\ 0 & 0 & 0 & 0 & 0 & a \\ 0 & 0 & 0 & b & -a & 0 \end{bmatrix} \begin{bmatrix} d_{200} \\ d_{020} \\ d_{002} \\ d_{100} \\ d_{010} \\ d_{001} \end{bmatrix} = \begin{bmatrix} 0 \\ 0 \\ 0 \\ 0 \\ 0 \\ 0 \end{bmatrix} \quad (60)$$

yielding $d_{001} = 0$ and leaving four linearly independent equations

$$\begin{aligned} d_{200}p + d_{020}q + d_{002}r &= 0 \\ -d_{020}a + d_{002}a + d_{100}p &= 0 \\ d_{200}b - d_{002}b + d_{010}q &= 0 \\ d_{100}b - d_{010}a &= 0 \end{aligned} \quad (61)$$

in the remaining five parameters, and making for one constant of motion.

- The skew-symmetric structure of the coefficient matrix

$$\begin{bmatrix} 0 & c & -b \\ -c & 0 & a \\ b & -a & 0 \end{bmatrix} \quad (62)$$

in the last three equations of Eq. (42) confers a zero determinant, so only two of these three equations are linearly independent. In subclasses where $a, b, c \neq 0$ the remainder of the equations are linearly independent, making for six equations in six unknowns and only a trivial solution to the invariants.

The invariants for the subclasses are plotted in Figure 3, along with numerically integrated trajectories starting from the initial condition $x(0) = [1 \ 1 \ 1]^T$. In general, only those subclasses enjoying two invariants have periodic solutions from any initial condition. The corresponding time-series of C_1 and C_2 , where they exist, are shown in SI Fig 3. Figure 3 of the paper illustrates three subclasses (2,3,7) where dynamics resides on a two-dimensional manifold, as the result of enjoying a single constant of motion. The absence of periodicity of these solutions is apparent from the relative thickness of these trajectories in the figure. Since the dynamics of these subclasses is circumscribed by the Poincaré-Bendixson theorem [21], we will not consider these further. Figure 3 also shows a subclass (4) that, like the general case, has no invariants as a result of all the linear coefficients being nonzero. Thus, relaxing the energy conservation constraint opens the door to much richer dynamics of the TVG, as illustrated below.

Table 3: Constants of motion for $p + q + r \neq 0$. Subclasses with three linear coefficients have no invariants, those with two linear coefficients have one quadratic invariant, and those with one or no linear coefficient have two independent quadratic invariants. The number of independent quadratic invariants is given by k .

No.	Subclass	C_1	C_2	C_3	k
1	$r = 0; b = c = 0$	$\frac{1}{2} \left(x_1^2 - \frac{p}{q} x_2^2 - \frac{p}{q} x_3^2 \right)$	$-\frac{p}{2a} x_3^2 + x_1$		2
2	$r = 0; c = 0$	$\frac{1}{2} \left(x_1^2 - \frac{p}{q} x_2^2 - 2\frac{a}{q} x_1 - 2\frac{b}{q} x_2 \right)$			1
3	$r = 0; b = 0$	$-\frac{1}{2} \frac{p}{a} x_3^2 + x_1 + \frac{c}{a} x_3$			1
4	$r = 0$				0
5	$a = b = c = 0$	$\frac{1}{2} \left(x_1^2 - \frac{p}{r} x_3^2 \right)$	$\frac{1}{2} \left(x_2^2 - \frac{q}{r} x_3^2 \right)$		2
6	$b = c = 0$	$\frac{1}{2} \left(x_1^2 - \frac{p}{q+r} x_2^2 - \frac{p}{q+r} x_3^2 \right)$	$\frac{1}{2} \left(\frac{pr}{(q+r)a} x_2^2 - \frac{pq}{(q+r)a} x_3^2 + 2x_1 \right)$		2
7	$c = 0$	$\frac{1}{2} \left(x_1^2 - \frac{p}{q} x_2^2 - 2\frac{a}{q} x_1 - 2\frac{b}{q} x_2 \right)$			1
8	$r = 0; a = b = c = 0$	$\frac{1}{2} \left(x_1^2 - \frac{p}{q} x_2^2 \right)$	$\frac{1}{2} x_3^2$		2
9	$r = 0; a = b = 0$	$\frac{1}{2} \left(x_1^2 - \frac{px_3 - c}{qx_3 + c} x_2^2 \right)$	$\frac{1}{2} x_3^2$		2

3 Chaos in the TVG

Where quadratic invariants do not exist for these 3-dimensional flows (Subclasses 4 and the general case) the dynamics are rich, and include irregular dynamics as well as chaos. We examine this further for subclass 4, for which we have examined a large ensemble of varying parameters and initial conditions using Latin hypercube sampling. Examples of irregular trajectories, their orbits and time-series of x_1 , are illustrated in SI Figs 4-5. We plot some of these cases in Figures 4-6. A minimal chaotic model in the TVG without energy conservation has

$$\begin{aligned}x_1' &= \rho x_2 x_3 + b x_3 - c x_2 \\x_2' &= (-\rho + \delta) x_3 x_1 + c x_1 - a x_3 \\x_3' &= a x_2 - b x_1\end{aligned}\tag{63}$$

where $q = -\rho + \delta$, so that $E' = \delta x_1 x_2 x_3$. Recall that with $\delta \neq 0$, there is no energy conservation. Since there are three linear feedbacks, this has no quadratic invariants (Table 3). Figure 4 shows the changing orbit sequence, for changing δ , including $\delta = 0$, for fixed a, b, c, ρ , and q calculated as $q = -\rho + \delta$. Corresponding time-series of x_1 and E are shown in Figures 5-6. The dynamics can become chaotic for nonzero δ . Energy is conserved only for $\delta = 0$ (Figure 6).

The particular example of $a = -0.67, b = 0.18, c = 0.70, \rho = 0.76$, and $q = -\rho + \delta$, is taken up further in Figure 7, which shows transient and stationary orbits for uniform increase in δ , from -0.25 to 0 . Poincaré sections (Figure 8) confirm the appearance of chaos for each of these cases except $\delta = -0.063$ and $\delta = 0$, and this is also confirmed by corresponding power spectral densities having continuous peaks (Figure 9), as well as positive finite-time Lyapunov exponents (Figure 10). Corresponding time-series are shown in SI Fig 6. These last examples serve to demonstrate that chaos can appear in the volume conserving TVG.

By analogy with subclass 4, for the full TVG with three quadratic terms we can write a model that admits chaos

$$\begin{aligned}x_1' &= \rho x_2 x_3 + b x_3 - c x_2 \\x_2' &= q x_3 x_1 + c x_1 - a x_3 \\x_3' &= (-\rho - q + \delta) x_1 x_2 + a x_2 - b x_1\end{aligned}\tag{64}$$

that also has non-conserved $E' = \delta x_1 x_2 x_3$ and no invariants in case of nonzero δ owing to three linear feedbacks. These systems in Eqs. (63)-(64) both preserve volume as the flow evolves.

In summary, a necessary condition for chaos in the volume-conserving TVG is the presence of three linear feedbacks (subclass 4 and the general case) along with two quadratic nonlinearities with nonzero δ as in subclass 4. We have not considered models with a single quadratic nonlinearity.

Table 4: Summary of the major symbols used.

Symbol	Definition
y_1, y_2, y_3	angular velocity of carrier body
K_1^2, K_2^2, K_3^2	principal moments of inertia of the gyrostat
h_1, h_2, h_3	angular momentum of the rotor relative to the carrier
E	kinetic energy: $E = \frac{1}{2} \sum_{i=1}^3 K_i^2 y_i^2$
M	squared angular momentum: $M = \frac{1}{2} \sum_{i=1}^3 (K_i^2 y_i + h_i)^2$
x_1, x_2, x_3	state variables of the TVG: $x_1 = K_1 y_1, x_2 = K_2 y_2, x_3 = K_3 y_3$
p, q, r	quadratic coefficients of TVG dynamics: $p = K_2^2 - K_3^2, q = K_3^2 - K_1^2, r = K_1^2 - K_2^2$
a, b, c	linear coefficients of TVG dynamics: $a = K_1 h_1, b = K_2 h_2, c = K_3 h_3$
$C_i(y_1, y_2, \dots, y_n)$	invariants of the system $\dot{y} = g(y)$, with $y = \begin{bmatrix} y_1 & y_2 & \dots & y_n \end{bmatrix}^T \in \mathbb{R}^n$ and $g: \mathbb{R}^n \rightarrow \mathbb{R}^n$
H	Jacobian of parameter transformation involved in VG->TVG
$d_{200}, d_{020}, d_{002}, d_{110}, d_{011}, d_{101}, d_{100}, d_{010}, d_{001}$	coefficients of quadratic invariants of TVG
d	vector of potentially non-zero coefficients: $d = \begin{bmatrix} d_{200} & d_{020} & d_{002} & d_{100} & d_{010} & d_{001} \end{bmatrix}^T$
B	matrix defining linear homogeneous equations satisfied by coefficients: $Bd = 0$
$C_1(x_1, x_2, x_3)$	first quadratic invariant of TVG (where it exists)
$C_2(x_1, x_2, x_3)$	second quadratic invariant of TVG (where it exists)
\mathcal{C}_1 and \mathcal{C}_2	surfaces describing the respective quadratic invariants
δ	$p + q + r$, which is nonzero in the absence of energy conservation

4 Summary and Discussion

The Volterra gyrostat (VG) and its transformation (TVG) appear ubiquitously within the structures of many low-order models (LOMs) [9, 4], and this paper provides a characterization of their quadratic invariants for each of the special cases discussed in [8] (Section 2). The present paper provides an explicit account of the expressions for quadratic invariants in the TVG and, given the close link between the number of invariants and the structure of these models, such inquiries are also relevant to identifying the conditions of chaotic dynamics in such models. We have shown how the number of invariants depends on the presence of the energy conservation constraint, as well as the number of linear feedback terms. The study shows that, since the TVG arises from a smooth transformation of variables it possesses two quadratic invariants in the presence of energy conservation, despite the parameter transformation not being invertible. Energy conservation corresponds to the quadratic coefficients in the TVG summing to zero. These invariants correspond to the same conservation laws as the VG even though they are not explicitly rendered as such; wherein energy and angular momentum and any affine transformation are conserved, giving periodic dynamics from any initial condition.

It is also shown that energy conservation is central to existence of two invariants of the TVG, and relaxing this constraint admits wider possibilities, from zero to two invariants. Such models without energy conservation also appear as the fundamental core of LOMs in weather and climate (e.g., [5]), and their characterization becomes important. The number of invariants in these more general models is related to the number of linear terms, with subclasses having three linear feedback terms possessing none. It is shown, in the absence of the energy conservation constraint, that subclasses with three linear coefficients have no invariants, those with two linear coefficients have one quadratic invariant, and those with one or no linear coefficient have two independent quadratic invariants (Section 2). Chaos can arise in the volume conserving flows with three linear feedback terms (Section 3).

The core of the paper (Section 2) is focused on estimating quadratic invariants in three state variables. We estimate the number of independent invariants that are consistent with the evolution equations of various subclasses of the TVG. Our study focuses on the gyrostat with two or more nonlinear terms. This reduces to estimating 6 coefficients, once we observe that for the TVG with at least two nonlinear terms the quadratic invariants cannot possess any mixed quadratic term. Then the number of quadratic invariants is related to the number of linearly independent solutions to a system of homogeneous linear equations (in these 6 unknown coefficients). These linear equations come from the consistency of the quadratic invariants with the evolution equations of the TVG. The analysis is repeated with and without the energy conservation constraint being present, clearly showing the relevance of energy conservation to the existence of a second invariant.

For these three-dimensional models the recognition of invariants, where they exist, obviates the need for explicit integration of the equations for understanding asymptotic as well as transient dynamics. Numerical investigations are of course important to identify the possibility of chaos, when no invariants exist. While we have not examined the existence of higher invariants of the model, the consistency of the numerical simulations with the number of quadratic invariants confirms the approach. We have numerically studied particular examples giving chaos when $\delta \equiv p + q + r \neq 0$. Circumscribing the possibilities for dynamics when this sum of quadratic coefficients δ is nonzero is an open problem. Since chaos cannot arise when

$\delta = 0$, it might serve naturally as a bifurcation parameter inviting further study. It is also important to consider the origin of nonzero δ in the conservative core of models having these structures (e.g. [5, 22]).

Previous authors have considered simple chaotic flows in three dimensions, where the simplicity of the model is usually characterized by fewer number of distinct terms defining the vector field. For example, [23] considered vector fields having five different terms (with two of them being nonlinear) or six terms (with one of them being nonlinear). These studies have illuminated the algebraically simplest chaotic models, most of which are dissipative, but there are examples of volume conserving flows too [23, 24, 25]. In fact, the simplest volume conserving chaotic flow in three dimensions has only four terms, of which two are nonlinear [25]. In comparison subclass 4 in Eq. (63) has eight terms, of which two are nonlinear, and thus is in no respect simple. Given that the present inquiry is confined to models having the gyrostat structure, and that we have not considered those subclasses with a single nonlinearity, we do not seek to identify simple chaotic models among more general vector fields. The importance of the models in Eqs. (63)-(64) lies in their origin in the gyrostat equations and thus ubiquity in the structure of LOMs. Therefore, the simplest chaotic flows within the family of gyrostats, and coupled gyrostats, merit inquiry despite them not being cataloged among the simplest chaotic flows across more general vector fields.

The famous LOM developed by Lorenz [3] of the Rayleigh-Benard problem of convective overturning in a fluid heated from below has been interpreted by Gluhovsky and Tong [8] as a forced-dissipative version of subclass 1 of the TVG where $p + q + r = 0$. The authors [8] show that this subclass has two integrals of motion. In the present study, we have shown that two integrals of motion are held by this subclass even if $p + q + r \neq 0$. The model of Lorenz has the same symmetry as its conservative core described here [3, 26], but its dynamics is very different [8], and for the LOM of [3] the conditions of chaotic dynamics arise from the combined effects of dissipation, which collapses volumes of initial conditions in phase space, and effects of forcing.

Analogously, for each of the subclasses of the TVG, a rich collection of quadratic LOMs can be conceived by extending these models to their forced and dissipative counterparts, whose dynamics might depart significantly from the models elucidated here. In general, with forcing and dissipation we might expect chaotic behavior to arise for each of the subclasses, regardless of the number of linear feedbacks. Moreover, subclass 4 and the most general case too will present chaos when forcing and dissipation are included, but the nature of the orbits will surely differ from those examined here. Since these LOMs shall in general depart from the TVG in respect of forcing, dissipation, as well as the presence of the energy conservation constraint, it is of interest to study the role of each of these factors on the resulting possibilities for dynamics in forced dissipative systems, and compare the mechanisms giving rise to chaos in each case.

Furthermore, the concept of VG with linear feedback has been extended to the generalized Volterra gyrostat having nonlinear feedback terms, which also arise naturally in low-order models [17]. It is of considerable interest to extend the present analysis to these models, to study their various invariants and the conditions permitting chaos. Ultimately, the TVG appears in low-order models not singly but as part of a system of a variety of different subclasses of the TVG that are coupled with each other. The underlying conservation laws, when they are stripped of forcing and dissipation, can generally possess quadratic invariants. Studying the invariants of systems of coupled TVGs, involving both linear and nonlinear feedback terms, is therefore a promising line of future inquiry. When derived from conservation laws we can expect such low-order

models to possess at most two (or a few) quadratic invariants. Considering the more general problem of invariants in systems of coupled gyrostats, as well as the conditions for chaos in these models can help illuminate the behavior of low-order models as well as the infinite-dimensional systems that they describe.

Acknowledgments

The authors are grateful to Frank Kwasniok, Vishal Vasan, and anonymous reviewers for helpful suggestions.

Declarations of interest

The authors have no competing interests to declare.

References

- [1] V. Volterra, “Sur la theorie des variations des latitudes,” *Acta Mathematica*, vol. 22, pp. 201–356, 1899.
- [2] J. Wittenburg, *Dynamics of Systems of Rigid Bodies*. Teubner Verlag, Stuttgart, 1977.
- [3] E. N. Lorenz, “Deterministic nonperiodic flow,” vol. 20, no. 2, pp. 130–141, 1963.
- [4] A. Gluhovsky, C. Tong, and E. Agee, “Selection of modes in convective low-order models,” *Journal of the Atmospheric Sciences*, vol. 59, pp. 1383–1393, 2002.
- [5] E. N. Lorenz, “Maximum simplification of the dynamic equations,” *Tellus*, vol. 12, pp. 243–254, 1960.
- [6] J. G. Charney and J. G. DeVore, “Multiple flow equilibria in the atmosphere and blocking,” *Journal of the Atmospheric Sciences*, vol. 36, pp. 1205–1216, 1979.
- [7] H. E. D. Swart, “Low-order spectral models of the atmospheric circulation: A survey,” *Acta Applicandae Mathematicae*, vol. 11, pp. 49–96, 1988.
- [8] A. Gluhovsky and C. Tong, “The structure of energy conserving low-order models,” *Physics of Fluids*, vol. 11, no. 2, pp. 334–343, 1999.
- [9] A. Gluhovsky and E. Agee, “An interpretation of atmospheric low-order models,” *Journal of the Atmospheric Sciences*, vol. 54, pp. 768–773, 1997.
- [10] A. Gluhovsky, “Energy-conserving and hamiltonian low-order models in geophysical fluid dynamics,” *Nonlinear Processes in Geophysics*, vol. 13, pp. 125–133, 2006.
- [11] F. Kwasniok, “The reduction of complex dynamical systems using principal interaction patterns,” *Physica D: Nonlinear Phenomena*, vol. 92, pp. 28–60, 1996.
- [12] F. Kwasniok, “Reduced atmospheric models using dynamically motivated basis functions,” *Journal of the Atmospheric Sciences*, vol. 64, pp. 3452–3474, 2007.
- [13] T. S. Amer, A. I. Ismail, and W. S. Amer, “Application of the Krylov-Bogoliubov-Mitropolski Technique for a Rotating Heavy Solid under the Influence of a Gyrostatic Moment,” *Journal of Aerospace Engineering*, vol. 25, pp. 421–430, 2012.
- [14] T. Amer, A. Galal, I. Abady, and H. Elkafly, “The dynamical motion of a gyrostat for the irrational frequency case,” *Applied Mathematical Modeling*, vol. 89, pp. 1235–1267, 2021.
- [15] J.-H. He, T. Amer, H. El-Kafly, and A. Galal, “Modelling of the rotational motion of 6-DOF rigid body according to the Bobylev-Steklov conditions,” *Results in Physics*, vol. 35, pp. 1–20, 2022.
- [16] S. Lakshmivarahan and Y. Wang, “On the structure of the energy conserving low-order models and their relation to Volterra gyrostat,” *Nonlinear Analysis: Real World Applications*, vol. 9, no. 4, pp. 1573–1589, 2008.

- [17] S. Lakshmivarahan and Y. Wang, “On the Relation between Energy-Conserving Low-Order Models and a System of Coupled Generalized Volterra Gyrostats with Nonlinear Feedback,” *Journal of Nonlinear Science*, vol. 18, pp. 75–97, 2008.
- [18] C. Tong, “Lord Kelvin’s gyrostat, and its analogs in physics, including the Lorenz model,” *American Journal of Physics*, vol. 77, pp. 526–537, 2009.
- [19] S. Lakshmivarahan, M. E. Baldwin, and T. Zheng, “Further analysis of Lorenz’s maximum simplification equations,” *Journal of the Atmospheric Sciences*, vol. 63, pp. 2673–2699, 2006.
- [20] P. J. Holmes and J. E. Marsden *Indiana University Mathematics Journal*, vol. 32, pp. 273–309, 1983.
- [21] J. Guckenheimer and P. Holmes, *Nonlinear Oscillations, Dynamical Systems, and Bifurcations of Vector Fields*. Springer, 1983.
- [22] R. B. Leipnik and T. A. Newton, “Double strange attractors in rigid body motion with linear feedback control,” *Physics Letters A*, vol. 86, pp. 63–67, 1981.
- [23] J. C. Sprott, “Some simple chaotic flows,” *Physical Review E*, vol. 50, no. 2, pp. R647–R650, 1994.
- [24] J. C. Sprott and S. J. Linz, “Algebraically simple chaotic flows,” *International Journal of Chaos Theory and Applications*, vol. 5, no. 2, pp. 1–20, 2000.
- [25] J. Heidel and Z. Fu, “Nonchaotic and chaotic behavior in three-dimensional quadratic systems: five-one conservative cases,” *International Journal of Bifurcation and Chaos*, vol. 17, no. 6, pp. 2049–2072, 2007.
- [26] R. Gilmore and C. Letellier, *The Symmetry of Chaos*. Oxford University Press, 2007.

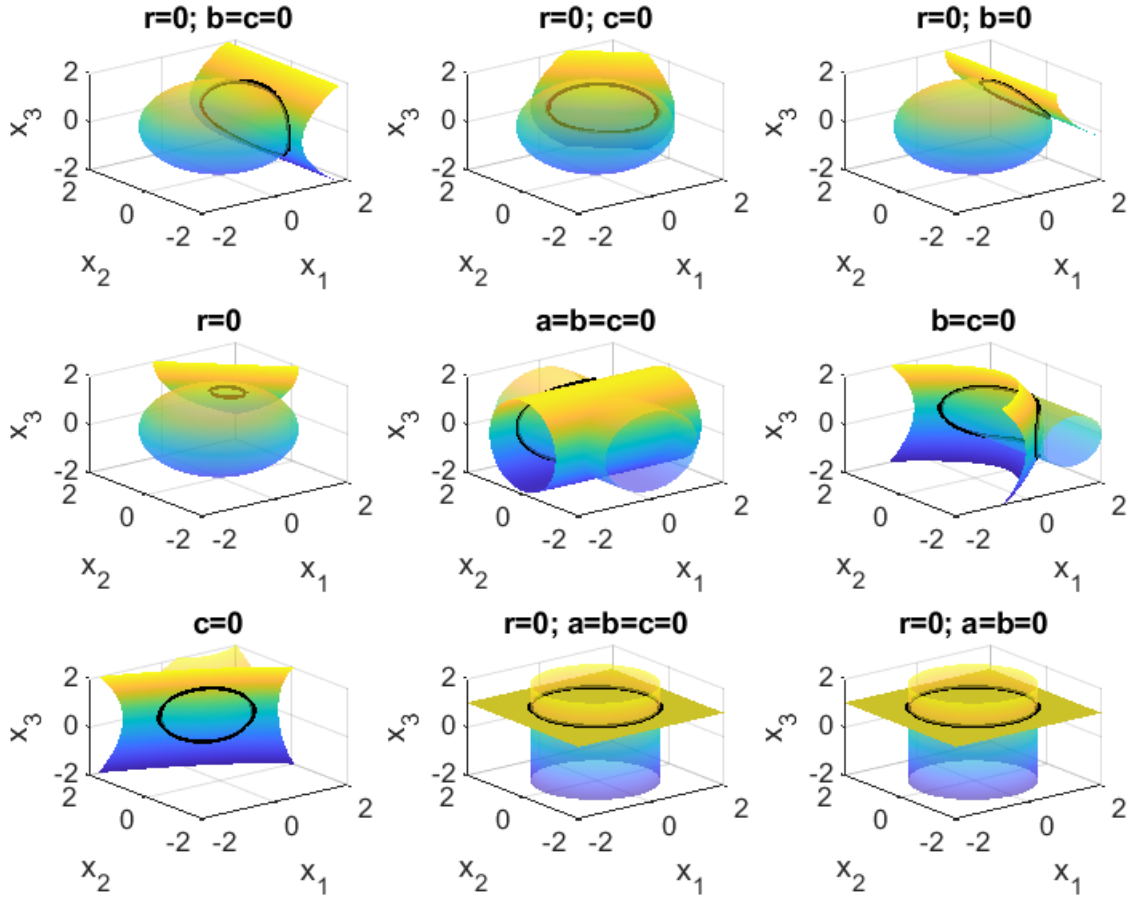


Figure 1: The two quadratic invariants for the TVG, for the subclasses ordered as in Table 1, and following [8]. The solid black curve shows corresponding solution trajectories of x , from numerical integration. Results are shown for the initial condition $x(0) = [1 \ 1 \ 1]^T$. These plots assume energy conservation $p + q + r = 0$, giving rise to periodic solutions.

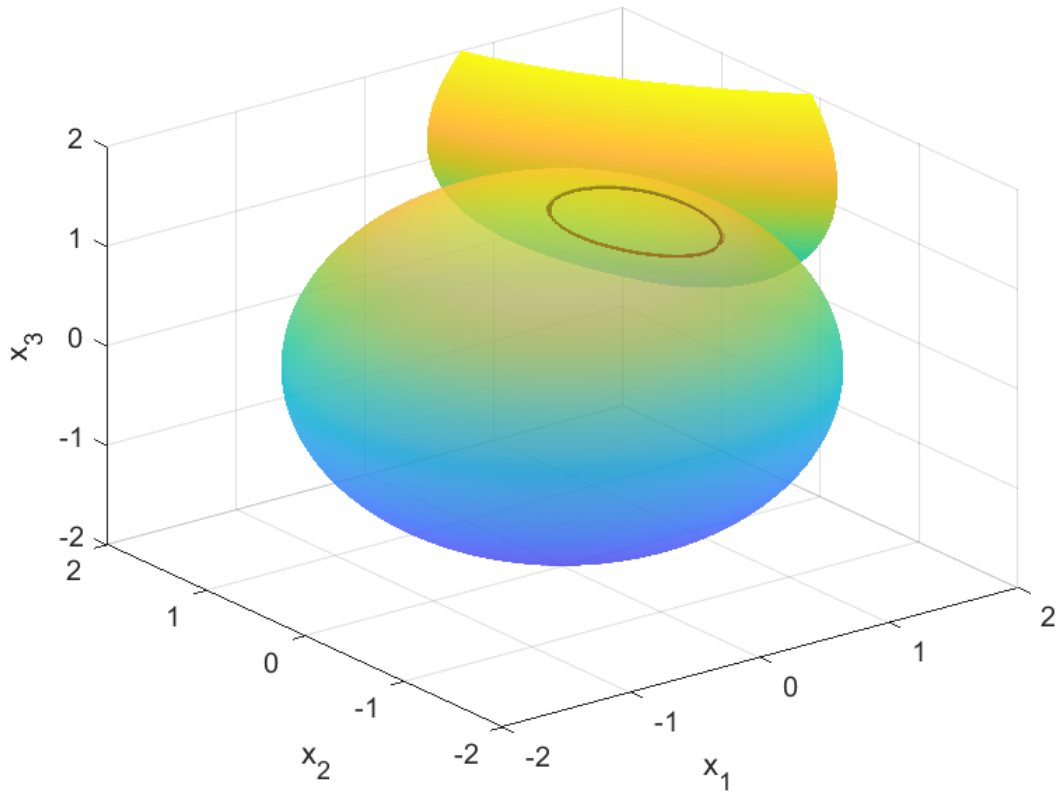


Figure 2: The two quadratic invariants for the Volterra gyrostat, in Eqs. (35) and (36). The solid black curve shows the solution trajectories of x , from numerical integration, for this general case. Results are shown for the initial condition $x(0) = [1 \ 1 \ 1]^T$.

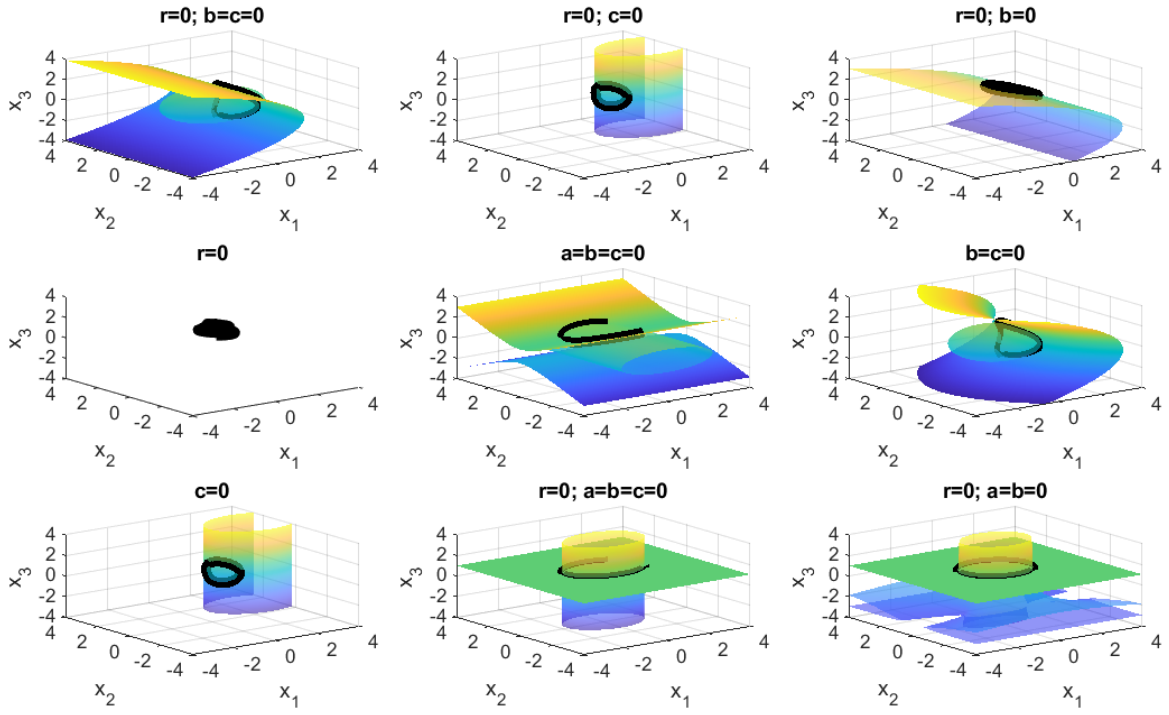


Figure 3: Constants of motion for the TVG for the subclasses ordered as in Table 3 in the absence of energy conservation, i.e. $p + q + r \neq 0$. The solid black curve shows corresponding solution trajectories of x , from numerical integration. Results are shown for the initial condition $x(0) = [1 \ 1 \ 1]^T$. Only those subclasses with two quadratic invariants (1,5,6,8,9) have periodic solutions.

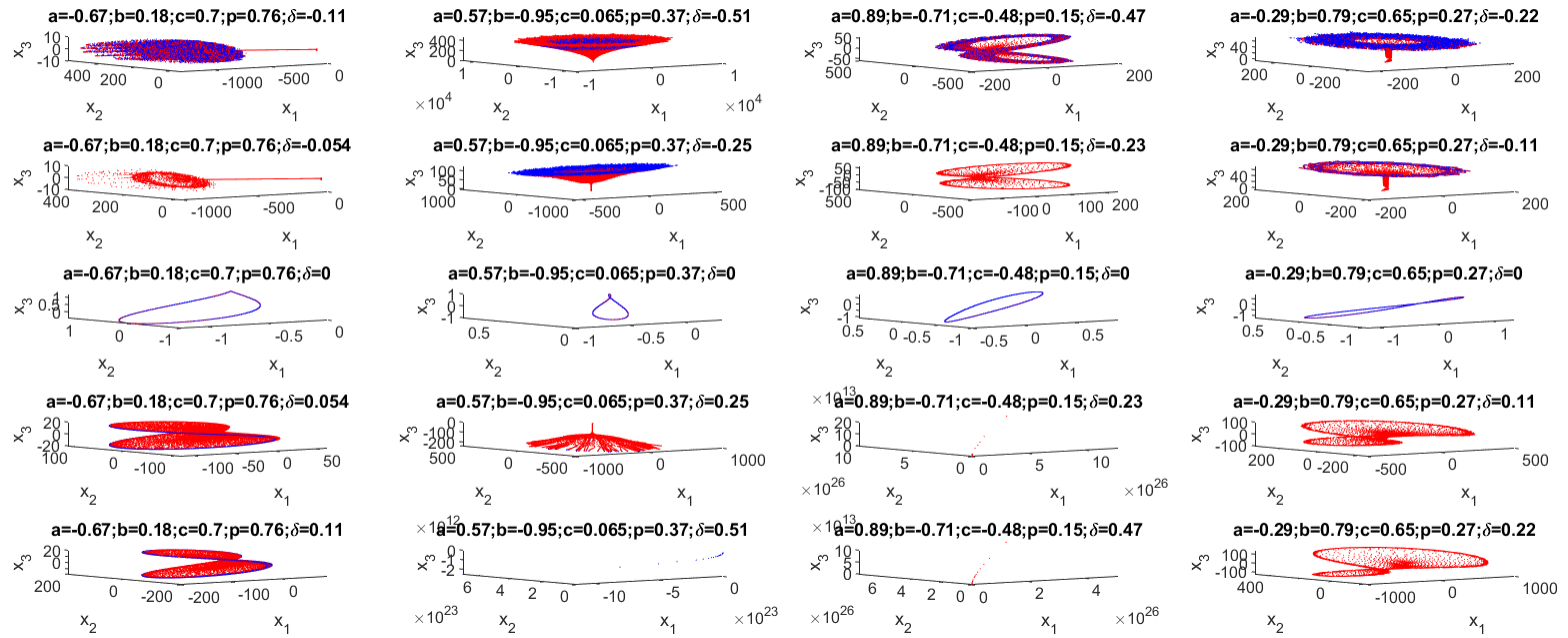
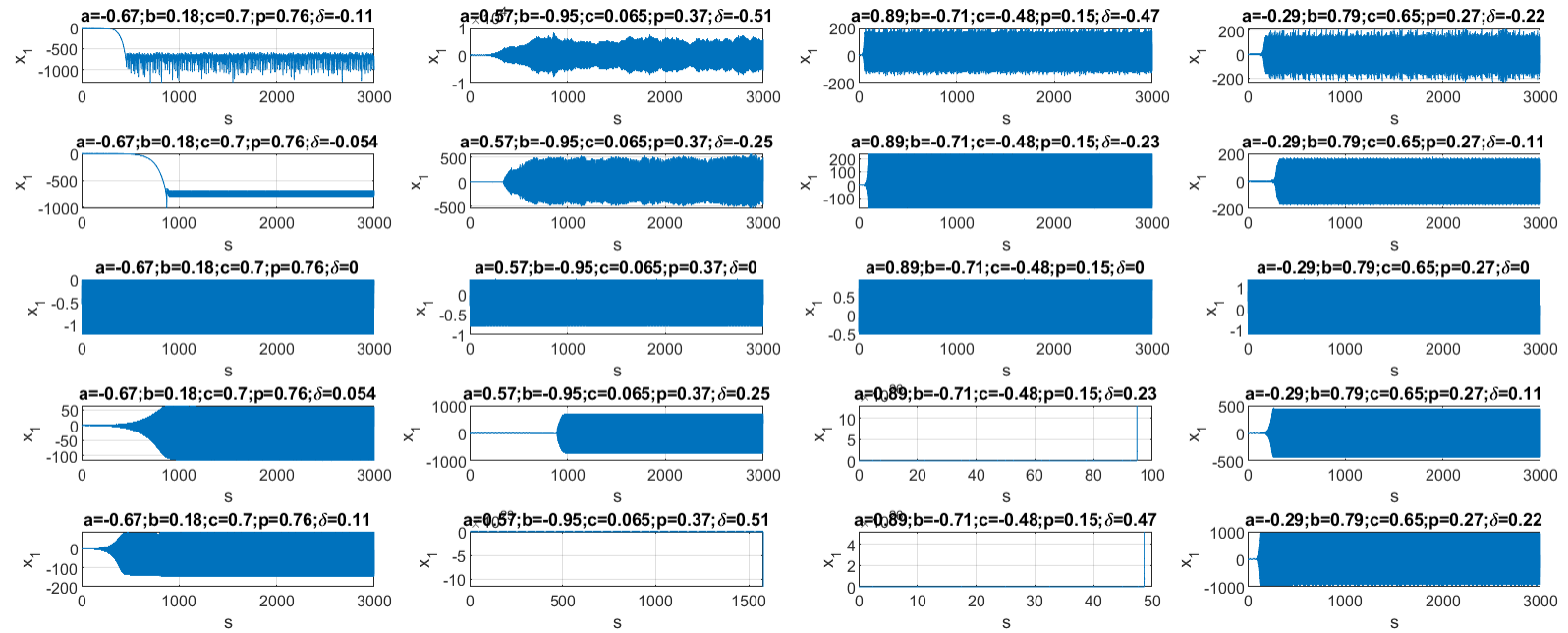


Figure 4: Orbits of subclass 4 ($r = 0$) without energy conservation, with each column showing results for fixed a , b , c , p , and q is calculated for each panel as $q = -p + \delta$, with δ varying by rows. Transient dynamics is shown in red and stationary orbit in blue. Corresponding time-series of x_1 and E are shown in Figures 5-6.

Figure 5: Time-series of x_1 for the orbits in Figure 4.

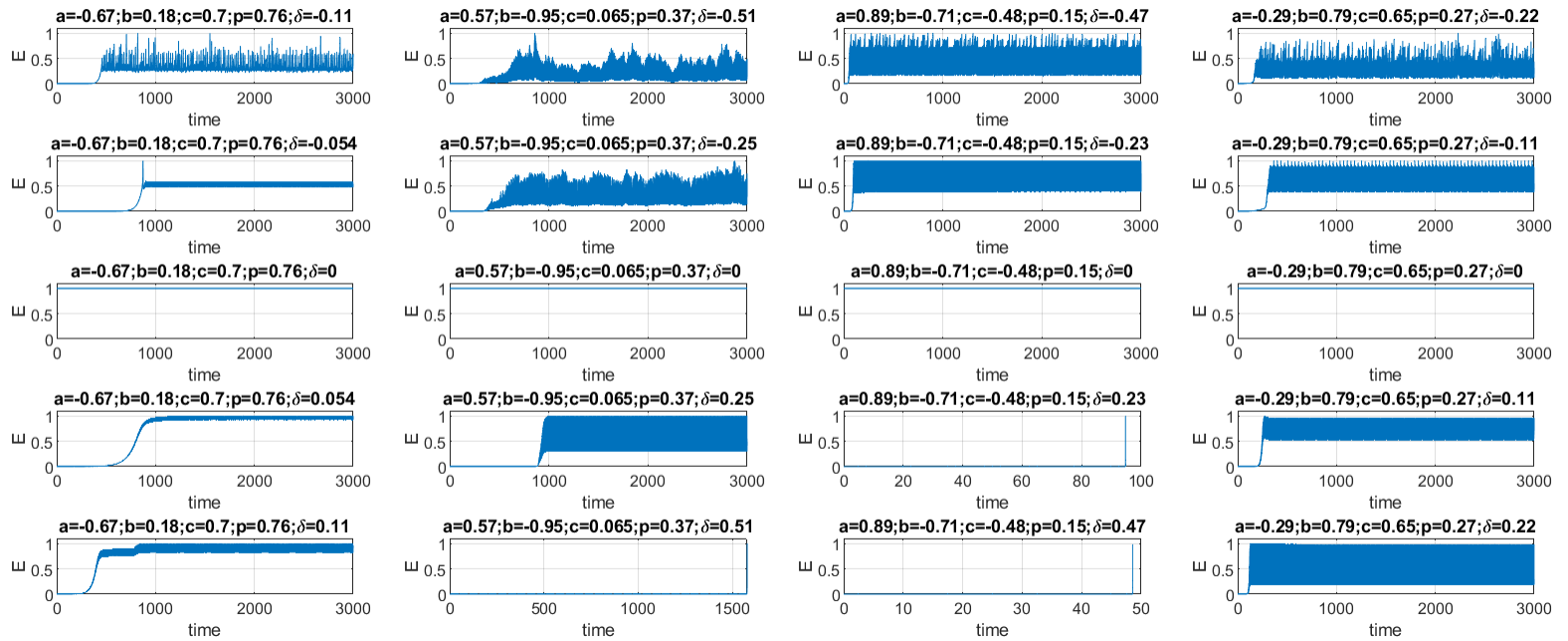


Figure 6: Time-series of E (normalized by its maximum value) for the orbits in Figure 4. E is constant only for $\delta = 0$ in the middle row.

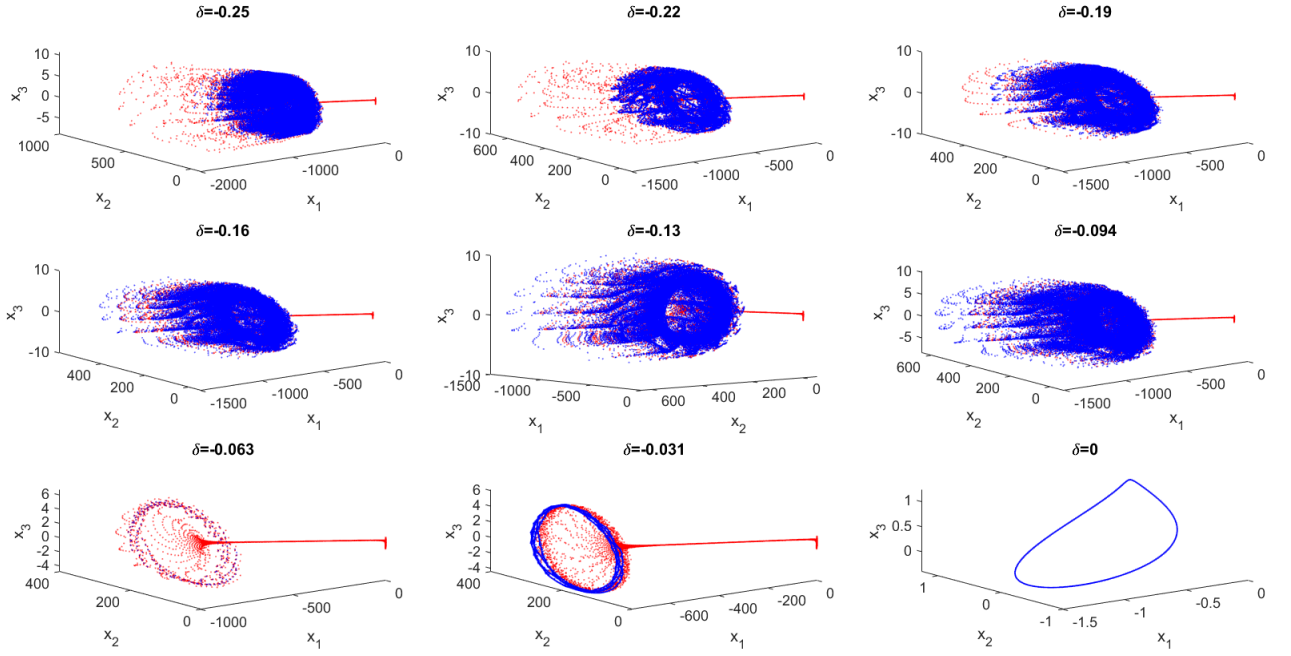


Figure 7: Orbits of subclass 4 ($r = 0$) without energy conservation, having $a = -0.67$, $b = 0.18$, $c = 0.70$, $p = 0.76$, and $q = -p + \delta$, as parameter δ is varied. Since $p + q = \delta$, energy conservation occurs only for $\delta = 0$. Successive panels show results for uniform increments of δ , where the stationary sequence is shown in blue. Chaos occurs in each of these cases except $\delta = -0.063$ and $\delta = 0$. Corresponding Poincaré sections are in Figure 8, power spectra in Figure 9, and Lyapunov exponents in Figure 10. SI Fig 6 shows time-series of x_1 .

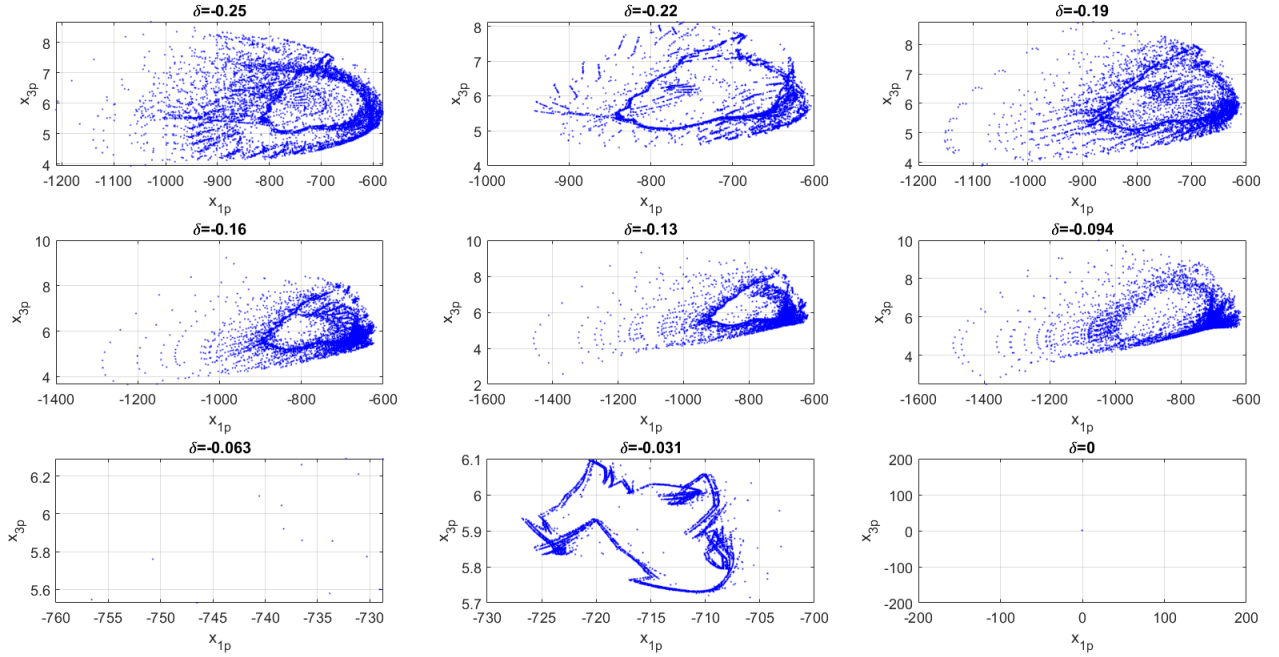


Figure 8: Poincaré sections of the stationary sequences (subclass 4) in Figure 7, demonstrating that chaos can occur for certain parameter values.

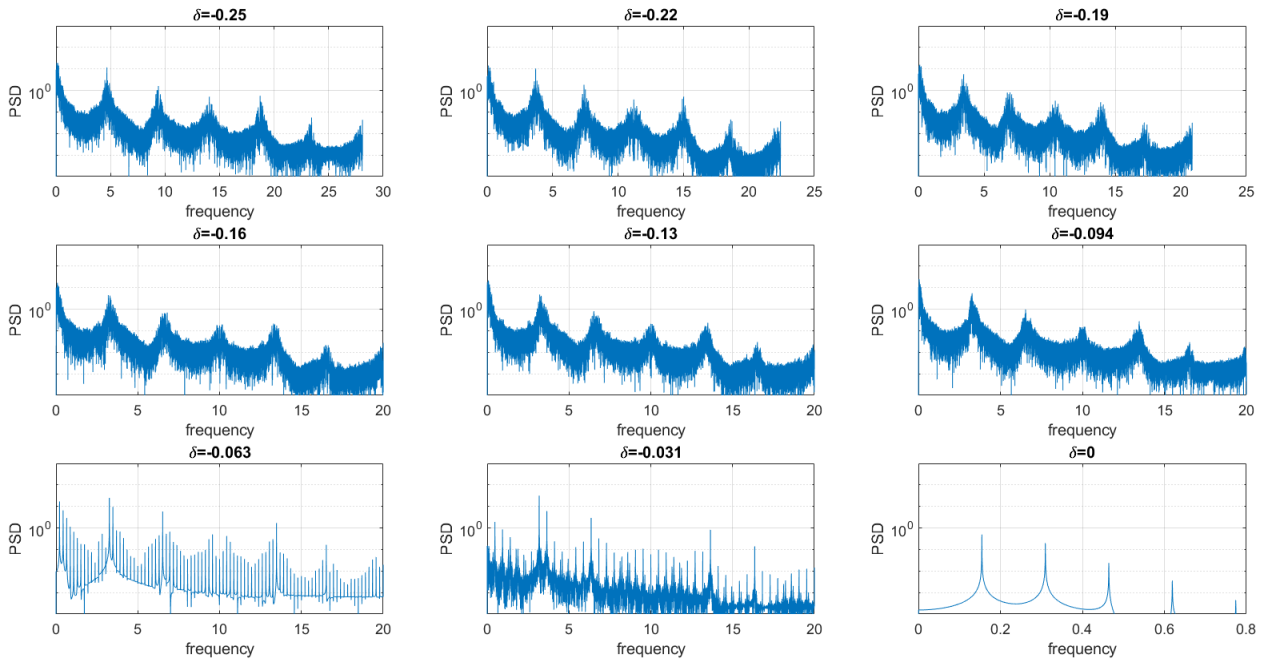


Figure 9: Power spectral density (log-scale) versus frequency (linear-scale) for stationary orbits in Figure 7, for subclass 4 without energy conservation, showing broadband spectra associated with chaos for certain parameter values.

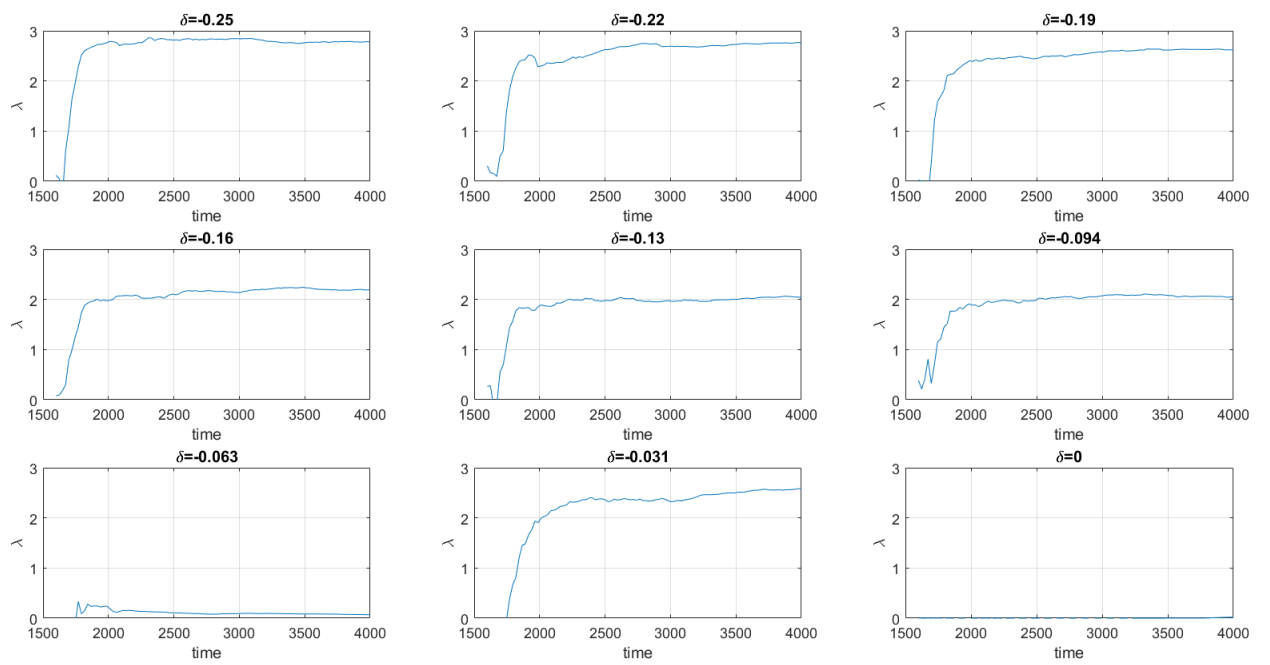


Figure 10: Evolution of finite-time Lyapunov exponent for stationary orbits in Figure 7, as a function of time s .